ACS APPLIED MATERIALS & INTERFACES

Research Article

www.acsami.org

Better Actuation Through Chemistry: Using Surface Coatings to Create Uniform Director Fields in Nematic Liquid Crystal Elastomers

Yu Xia,[†] Elaine Lee,[†,‡] Hao Hu,[†] Mohamed Amine Gharbi,[†,§] Daniel A. Beller,[∥] Eva-Kristina Fleischmann,[⊥] Randall D. Kamien,[§] Rudolf Zentel,[⊥] and Shu Yang*[,†]

[†]Department of Materials Science and Engineering, University of Pennsylvania, 3231 Walnut Street, Philadelphia, Pennsylvania 19104, United States

[‡]Engineering Directorate, Lawrence Livermore National Laboratory, 7000 East Avenue, Livermore, California 94550, United States

[§]Department of Physics and Astronomy, University of Pennsylvania, 209 South 33rd Street, Philadelphia, Pennsylvania 19104, United States

[∥]Paulson School of Engineering and Applied Sciences, Harvard University, 29 Oxford Street, Cambridge, Massachusetts 02138, United States

[⊥]Institute of Organic Chemistry, Johannes Gutenberg-Universität Mainz, Duesbergweg 10−14, 55128 Mainz, Germany

Supporting Information

ABSTRACT: Controlling the molecular alignment of liquid crystal monomers (LCMs) within nano- and microstructures is essential in manipulating the actuation behavior of nematic liquid crystal elastomers (NLCEs). Here, we study how to induce uniformly vertical alignment of nematic LCMs within a micropillar array to maximize the macroscopic shape change using surface chemistry. Landau−de Gennes numerical modeling suggests that it is difficult to perfectly align LCMs vertically in every pore within a poly(dimethylsiloxane) (PDMS) mold with porous channels during soft lithography. In an untreated PDMS mold that provides homeotropic anchoring of LCMs, a radially escaped configuration of LCMs is observed. Vertically aligned LCMs, a preferred configuration for actuation, are only observed when using a PDMS mold with planar anchoring. Guided by the numerical modeling, we coat the PDMS mold with a thin layer of poly(2-hydroxyethyl methacrylate) (PHEMA), leading to planar anchoring of LCM. Confirmed by polarized optical microscopy, we observe monodomains of vertically aligned LCMs within the mold, in agreement with modeling. After curing and peeling off the mold, the resulting NLCE micropillars showed a relatively large and reversible radial strain (~30%) when heated above the nematic to isotropic transition temperature.

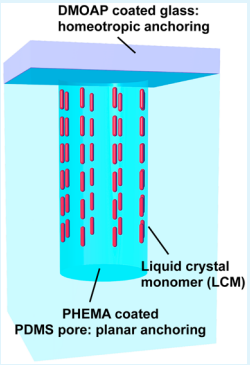

KEYWORDS: *liquid crystal elastomer, surface chemistry, monodomain, soft lithography, actuator*

INTRODUCTION

Because of their geometrical, mechanical, and electronic anisotropy, liquid crystal (LC) molecules are not only highly sensitive to external aligning fields but can also exquisitely control the propagation of electromagnetic phenomena. Consequently, LC molecules have long been of interest for scientific advancement and technological applications, including displays, artificial muscles, and actuators that rely upon anisotropic properties of LC molecules.[1−8] It is known that nematic liquid crystalline elastomers (NLCEs) exhibit a spontaneous contraction along the director axis when heated above their nematic (N)−isotropic (I) phase-transition temperatures (T_{NI}), and the polymer chain adopts, on-average, a spherical conformation.[9] Therefore, NLCEs have a reversible shape memory effect when triggered by external stimuli, including heat, light, and electric fields.[10−14] However, the deformation of NLCE networks is highly dependent on the molecular alignment of LCs, both globally and locally, on the boundary conditions imposed at interfaces by topography, topology, and surface chemistry, as well as on the application of the external field.[12]

Coupling of responsive materials with patterned surfaces at the micro- and nanoscale has led to interesting surface properties, including tunable structural color and transparency,[15−20] tunable dry adhesion,[21−23] and switchable wettability.[24−26] To achieve a large and reversible strain in microstructured NLCE actuators,[10−14] it is critically important to control LC anchoring within the pattern at the molecular level. The most common techniques to control LCM alignment microscopically include rubbing the substrate and application of a magnetic field before the LCMs are cross-linked. While rubbing using a velvet cloth is effective on a flat surface by generating microgrooves to align LC molecules,[12,27,28] it is not possible to apply this macroscopic method to create grooves against a topographic substrate of height variations, more specifically, in a soft lithography mold with porous channels, which has been commonly used to prepare micro- and nanostructured polymers. Moreover, the generation of static

Received: March 5, 2016
Accepted: April 29, 2016
Published: May 6, 2016

DOI: 10.1021/acsami.6b02789
ACS Appl. Mater. Interfaces 2016, 8, 12466−12472

charge and scratches will interfere with the LC alignment within the microgrooves.

To address this challenge, Keller et al. first demonstrated the use of a magnetic field (1−1.5 Tesla) to align LCMs vertically along the film thickness within the poly(dimethylsiloxane) (PDMS) mold with cylindrical pores (20 μm in diameter and 100 μm in height).[29,30] After curing, they obtained NLCE micropillar arrays and demonstrated a large contraction strain (~35%) when actuating the micropillars made of side-chain NLCEs[29] above T_{NI} (120 °C). Nevertheless, LCM alignment was not confirmed by polarized optical microscopy (POM) in the early reports. Since the reports, the magnetic alignment method has been widely adopted in many LCM systems, yet detailed investigation (both experimentally and theoretically) of LCM anchoring within a soft lithography template such as PDMS mold remains lacking. In part it is because, compared to a flat substrate, micropatterned PDMS molds provide much more complicated surface topographies to control the LCM anchoring uniformly over the entire sample area−so-called monodomain LC anchoring. When the dimension of the mold shrinks to (sub)micron size, the surface effects (e.g., surface chemistry, surface energy) become increasingly important to control the LC alignment. In addition, depending on the field strength and how the magnetic field is applied, there will always be a field gradient across the sample thickness and on an $x-y$ plane, which in turn will impact the uniformity of the LC director field throughout the sample, and the achievable actuation strain level. Given the wide range of potential applications of structured NLCEs, it is pressing to understand and eventually precisely control LCM anchoring within a PDMS mold during soft lithography.

Here, we prepared NLCE micropillars (diameter of 10 μm, pitch of 20 μm, and height of 40 μm) by aligning the NLC monomer, (4″-acryloyloxybutyl)-2,5-di(4′-butyloxybenzoyloxy) benzoate (LCM4), in a surface-treated PDMS mold, followed by UV curing. To generate a uniform, defect-free monodomain nematic configuration of vertically aligned LCM4 within the pores, it is important to promote planar anchoring of LCM4 inside the mold. We investigated the LCM4 alignment under POM using small molecule NLC, 4-cyano-4′-pentylbiphenyl (5CB), as reference. The results were corroborated with Landau−de Gennes numerical modeling, which simulated the LC alignment within the PDMS mold with both homeotropic and planar anchoring. In all cases, we found that perfect alignment of the LC director field along the pillar thickness could only be achieved with planar anchoring surface chemistry. To confirm this experimentally, we coated a thin layer of poly(2-hydroxyethyl methacrylate) (PHEMA) onto the PDMS mold to create degenerate planar surface anchoring for both LCM4 and 5CB. In comparison, in untreated PDMS molds, both NLCs maintained homeotropic anchoring at the interfaces and the director exhibited radial escape into the third dimension.[31] The NLCE pillars with planar anchoring demonstrated a relatively large radial strain (~30%) during heating across T_{NI}, while those created with homeotropic alignment had smaller strains due to the inherent frustration of the nematic texture within the pillars.

EXPERIMENTAL SECTION

Materials. (4″-acryloyloxybutyl)-2,5-di(4′-butyloxybenzoyloxy)-benzoate (LCM4) was synthesized according to the literature.[3] *N*,*N*-dimethyl-*n*-octadecyl-3-amino-propyltrimethoxysilyl chloride (DMOAP), hydroxyethyl methacrylate (HEMA), 1,6-hexane-diol diacrylate and 4-cyano-4′-pentylbiphenyl (5CB) were purchased from Sigma-Aldrich and used as received. Photoinitiator Irgacure184 (1-hydroxy cyclohexyl phenyl ketone) was obtained from Ciba Specialty Chemicals.

Preparation of PDMS Molds. The PDMS porous membrane (diameter of 10 μm, pitch, or center-to-center distance of 20 μm, and depth of 40 μm) was replicated from the epoxy (D.E.R. 354, Dow Chemical) pillar master, following the protocol reported earlier.[32]

Preparation of PDMS Molds with Different Surface Chemistry. The as-cured PDMS porous membranes offered homeotropic anchoring to LCM4 and 5CB, and were used as control substrates. To prepare a planar anchoring surface, the PDMS mold was immersed into a solution consisting of Irgacure184 (30 wt %) in acetone for 30 min, followed by rinsing with acetone three times and drying by air gun. The PDMS mold was then immersed into neat HEMA liquid and exposed under UV light (365 nm, Hg lamp) at a dosage of 1000 mJ/cm^2. The resulting mold was rinsed by ethanol three times to remove unreacted HEMA monomers, followed by drying on a hot stage at 95 °C.

Preparation of DMOAP-Coated Glass substrates. Glass slides were precleaned by washing with ethanol and acetone twice, respectively. They were then immersed into an aqueous solution of DMOAP (1 vol %) for 30 min, followed by rinsing with DI water three times and baking at 110 °C in an oven for 1 h.

Preparation of 5CB in the PDMS Mold. One drop of 5CB (~5 μL) was placed on the precleaned glass slide, and the PDMS mold (treated or untreated) was applied on top. After filling the mold with 5CB by capillary force for 1 min, the PDMS mold was lifted and bladed with a razor blade on the top surface to remove the residual 5CB. Then, a DMOAP treated glass slide was placed on top of the PDMS mold, and the sample filled with 5CB was characterized by POM.

Fabrication of LCM4 Pillars. LCM4 and 1,6-hexanediol diacrylate (as a cross-linker) were first mixed at a molar ratio of 4:1 in dichloromethane (20 wt %) to obtain a homogeneous solution, followed by addition of 2 wt % of photoinitiator (Irgacure 184). Next, 20 μL of the mixture was drop-cast on a clean glass slide and dried under vacuum. The mixture was then covered by the PDMS mold heated to 110 °C on a hot stage for 10 min. After the pores of the mold were completely filled with LCM4, the glass slide was carefully removed, and a razor blade was used to scrape off the residual LCs. The PDMS mold filled with LCM4 was then placed on a DMOAP treated glass substrate, and examined under POM to check LC anchoring before UV exposure. The PDMS mold along with LC monomers was exposed to 365 nm UV light (97435 Oriel Flood Exposure Source from Newport, intensity of 54 mW/cm^2) at 17 000 mJ/cm^2 dosage, followed by removal of the DMOAP coated glass substrate. The sample was then placed on top of a thin layer of polyurethane acrylate (PUA) liquid (Minuta Technology) on a clean glass slide, and exposed with another 17 000 mJ/cm^2 dosage of UV light to bond PUA onto pillars. After the sample was cooled to room temperature, the PDMS mold was peeled off to obtain the NLCE pillars supported on a PUA thin film. Here, the PUA supporting layer (more rigid than PDMS) helps to pull the LCE pillars out of the PDMS mold, much like the use of poly(methyl methacrylate) (PMMA) layer in the literature.[13]

Characterization. The LC textures were observed by an Olympus BX61 motorized optical microscope with crossed polarizers using CellSens software. Water contact angle was measured from a 5-μL water droplet placed on a flat PDMS film coated with PHEMA polymerized at different UV dosages using a model 200 Ramé−Hart standard automated goniometer with sessile drop method. The water contact angle was averaged over three measurements at different locations of the sample. The size of LCM4 pillars was measured using optical microscopy (Olympus BX61) in the bright field (BF) mode. The diameter of each pillar across the top was measured and averaged over all the pillars in Figure 4e. In the horizontal direction, pillars were carefully pushed down to the supporting substrate by applying a gentle sheer force on the top of the pillars using a glass slide, followed by measuring the pillar size across the middle of each pillar before and

DOI: 10.1021/acsami.6b02789
ACS Appl. Mater. Interfaces 2016, 8, 12466−12472

after heating, respectively (Figure 4c,d). The reported sizes of the pillars were averaged over all the pillars shown in Figure 4c–e.

Landau–de Gennes Numerical Modeling. Numerical modeling of LC alignment within the PDMS mold was performed on 5CB as a model LC according to literature[33] using the Frank elastic constants of 5CB at 298 K,[34] $K_1 = 0.64 \times 10^{-11}$ N (splay), $K_2 = 0.3 \times 10^{-11}$ N (twist), and $K_3 = 1 \times 10^{-11}$ N (bend). The simulation box to model 5CB in cylindrical pores was set as diameter 352 nm and height 1408 nm; the size is smaller than experiments due to the calculation time. The aspect ratio (height/diameter) of the pores is 4, the same as that in the sample.

RESULTS AND DISCUSSION

As mentioned earlier, to fabricate monodomain NLCE microstructures by soft lithography, researchers mainly rely on the magnetic field to align LCMs using a nontreated PDMS mold.[13,29,30,35] The freshly prepared PDMS surface has a low surface energy (~20 mJ/m^2). The commonly used small molecule NLC, e.g. 5CB, has weak homeotropic anchoring on the PDMS surface. To understand the effect of surface chemistry in aligning NLCs, we first simulated the anchoring of 5CB in a PDMS pore using Landau–de Gennes numerical modeling. As seen in Figure 1, 5CB filled in the untreated

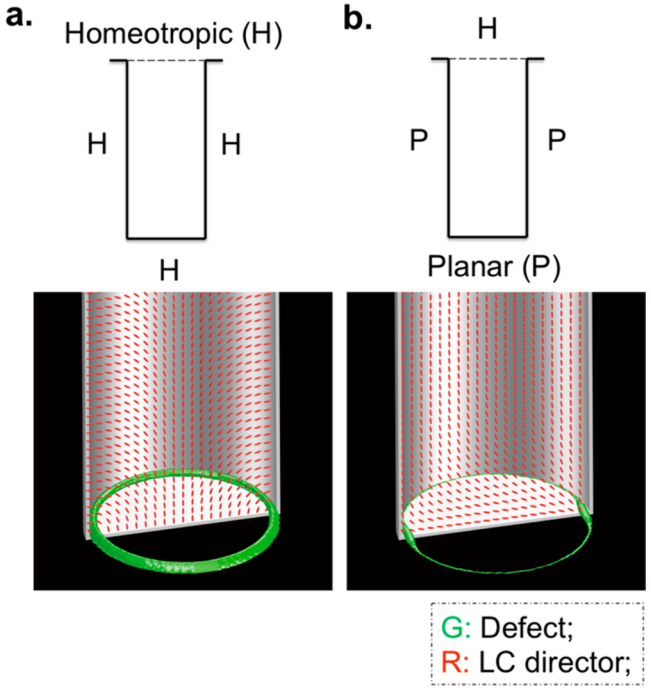

Figure 1. Landau–de Gennes numerical modeling of 5CB in a PDMS mold with (a) homeotropic anchoring and (b) planar anchoring.

PDMS mold adopts the classic radial escape into the third dimension (Figure 1a). To achieve full vertical alignment of the director in the PDMS pore, we used an external magnetic field. The effect of a magnetic field can be quantified by the magnetic coherence length, ξ_H, the length scale over which the LC director can orient and reorient along the field direction, given by

$$\xi_H = \sqrt{\frac{K_3}{\Delta\chi H^2}} \quad (1)$$

where K_3 is the bend elastic constant of LC, $\Delta\chi$ is the anisotropic magnetic susceptibility, and H is the magnetic field strength. In the case of a small molecule LC such as 5CB, K_3 is on the order of 10^{-11} N and $\Delta\chi$ is on the order 10^{-7}.[36] Thus, with a magnetic field strength $H \sim 1$ T, 5CB with any boundary conditions can be reoriented on a length scale $\xi_H \sim 10$ nm. Therefore, a strong magnetic field could be quite effective in aligning 5CB molecules into monodomains in the PDMS pores. However, this is not the case for NLC monomers such as LCM4, which often fail to be fully aligned within the pores under the magnetic field. Radially escaping configurations of LCM4 in PDMS pores under an 1.5 T vertical magnetic field have been reported.[13] However, the exact mechanism remains unclear, since neither the elastic constants of LCM4 nor its magnetic susceptibility has been precisely measured. Recall that in the NLCEs, there is different shape transformation parallel and perpendicular to the local director field. Thus, in the escaped configuration, large strains cannot be achieved because of the radial variation of the LC texture. With our desire to create pillars with a large strain response when heated across T_{NI}, we seek, instead, a nematic texture that generates a cooperative shape transformation. However, planar anchoring alone on the PDMS mold surface presents a potential problem—the bottom of a cylindrical pore would disfavor a uniform nematic texture parallel to the cylinder axis. Our numerical modeling, however, finds that this issue is limited to the bottom of the pore for 5CB (Figure 1b). If we can create and maintain this nematic texture in LCM4 during photopolymerization, it is possible to achieve a large strain without the use of an aligning magnetic field—purely through interfacial chemistry!

Indeed, when we grafted a thin layer of PHEMA on the PDMS mold we induced planar anchoring of the LCs (Figure 2a). While planar anchoring of LCMs on a glass slide is usually achieved by coating a thin layer of poly(vinyl alcohol) (PVA) or polyimide (PI) on the substrate, it is challenging to uniformly coat hydrophilic polymers (i.e., PVA or PI) on a hydrophobic PDMS mold. To circumvent this, we first treated the mold with an acetone solution of photoinitiator (Irgacure184), which we expected to be partially trapped within the mold surface (since PDMS is slightly swollen by acetone with a swelling ratio ~1.03[37]). The PDMS mold was then immersed into HEMA monomers that wet the PDMS surface, followed by UV curing at different dosages to ensure complete coverage of PHEMA on the PDMS mold as confirmed by water contact angle results at different UV curing dosage (Figure S1). At a low UV dosage (≤800 mJ/cm^2), the water contact angle of the mold was greater than 50°. At 1000 mJ/cm^2, the smallest water contact angle (~27°) was achieved, suggesting sufficient coverage and polymerization of PHEMA on PDMS. At a higher dosage (1500 mJ/cm^2), the water contact angle increased again, possibly due to condensation/cross-linking of the hydroxyl groups on PDMS. The cured PHEMA has very similar chemistry to PVA as they both have one hydroxyl group per repeat unit.

We then investigated the anchoring of 5CB and LCM4 in the PDMS molds under POM. We used 5CB to establish baseline expectations. As predicted by numerical modeling (Figure 1), 5CB in the PDMS mold attains an escaped configuration under homeotropic anchoring and vertical alignment under planar alignment. As sketched in Figure 3a, alignment of 5CB should generate two disclination loops at the top edge and bottom corners of the mold. The escaped configuration has lower energy and will appear as a ± 1 planar defect under POM – the standard four-brush texture, as shown in Figure 3b. Under

DOI: 10.1021/acsami.6b02789
ACS Appl. Mater. Interfaces 2016, 8, 12466–12472

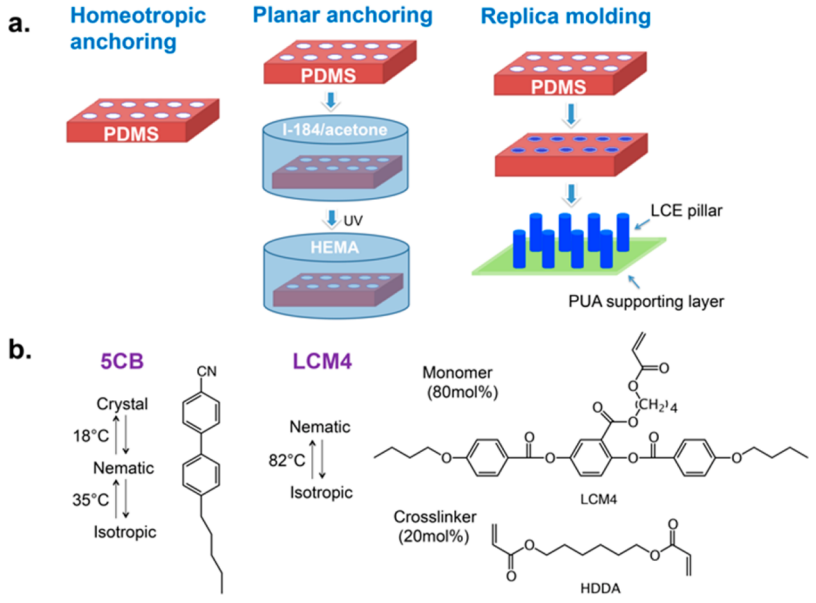

Figure 2. (a) Schematic illustrations of the preparation of the PDMS molds with different surface chemistry and the fabrication of LCE pillar array. Pillar dimensions: diameter, 10 μm; pitch (center-to-center distance), 20 μm; and height, 40 μm. (b) Chemical structures of LC systems used in the experiments.

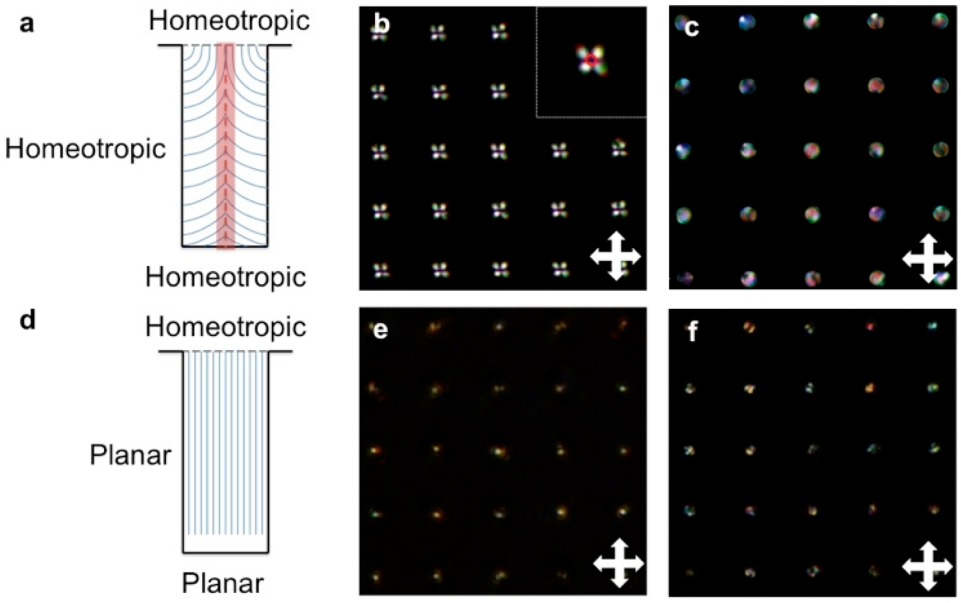

Figure 3. (a) Schematic of the LC director in a mold with homeotropic anchoring. The red dotted line indicates the escape of the LC director, while the red shaded region indicates the width of the escaping configuration, where the director field is uniformly vertical. POM images of (b) 5CB and (c) LCM4 under homeotropic anchoring in the nontreated PDMS mold. (b, inset) LC escaping domain indicated by the red circle under cross polarizers when observing the sample from the top under POM. (d) Schematic of the LC director in a PDMS mold treated with planar anchoring chemistry. POM images of (e) 5CB and (f) LCM4 in a planar-anchored PDMS mold treated by PHEMA.

planar anchoring, the numeric suggests that 5CB molecules will be mostly vertically aligned with director distortion only occurring at the bottom of the mold but with no disclination line on the top edge (Figure 3d). Thus, under POM, the image should be dark with light transmitted only from the distorted LC director at the bottom of the mold (see detailed LC director field in Figure 1b), in agreement with the experimental observation (Figure 3e).

We now turn to LCM before polymerization. In the case of homeotropic anchoring, a polydomain texture lacking a simple cross with each pore was observed under POM (Figure 3c and Figure S2) as a result of non-uniform light transmittance. It has been reported that the standard escaped radial structure can be achieved by applying a vertical magnetic field from a 1.5T permanent magnet.[13] Fortunately, in the case of planar anchoring (Figure 3f) we achieved the target texture, and a match to that of 5CB as seen in Figure 3e.

So do we get the desired effect? We carefully cross-linked LCM4 within the mold under planar anchoring and POM observation confirmed that monodomain alignment of LCM4 within the pillars was maintained. The tops of the extracted pillars now showed the texture on the bottom of the PDMS

DOI: 10.1021/acsami.6b02789
ACS Appl. Mater. Interfaces 2016, 8, 12466−12472

mold, revealing topological defects seen in Figure 4a,b. To better understand the LCM4 alignment within the mold and

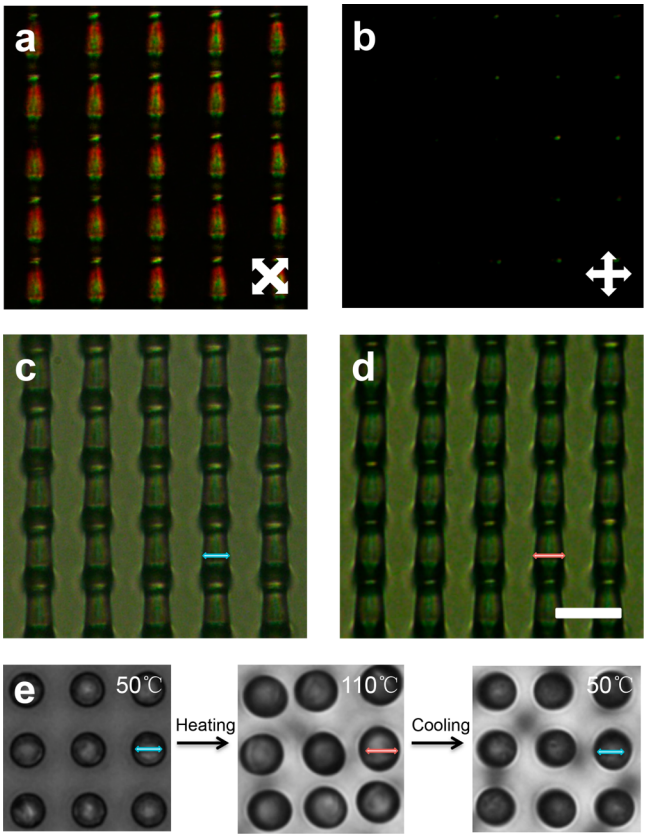

Figure 4. Cross-sectional POM images of LCM4 pillars after UV curing viewed at (a) 45° and (b) 0° polarization angles. Cross-sectional views of bright field (BF) images of LCM4 pillars at (c) 50 °C and (d) 110 °C. (e) Top-view BF image of LCM4 pillars through a heating and cooling cycle. Blue and red arrows in panels c–e indicate the position of pillars for measurement of diameter at 50 and 110 °C, respectively. Diameter of the micropillar was measured and averaged from all pillars in panels c–e: blue (50 °C), 8.5 ± 0.2 μm; red (110 °C), 11.1 ± 0.2 μm.

how these defects were formed when LCM4 infiltrated the PDMS mold, we performed Landau–de Gennes numerical modeling of 5CB. As seen in Figure 5, the observed defects arise from the planar anchoring of the LCs to the PDMS mold at the bottom of each pore. When planar anchoring is weak (Figure 5a), no defect appears either in the bulk or at the boundary. When planar anchoring strength is increased (Figure 5b–d), defects start to arise from the corner of the pore: the line defect at the corner (Figure 5b) gradually shrinks down to two point defects, as seen in Figure 5d). Experimentally, we see line defects at the corner from 5CB in the planar anchored PDMS mold (Figure 6a), a configuration close to the simulation result in Figure 5b, indicating that the two systems have similar surface anchoring contributions to the LC director orientation. Therefore, we can estimate the surface anchoring strength of 5CB in PHEMA treated PDMS pores from simulation. Because the simulation box is ~30 times smaller than the actual pore size in experiment, the experimental data suggests that the planar anchoring strength for 5CB in a PHEMA treated pore is roughly $\frac{7.74\times10^{-4}\,\mathrm{J/m^2}}{30} \sim 10^{-5}$ J/m^2. Because 5CB and LCM4 showed similar anchoring config-

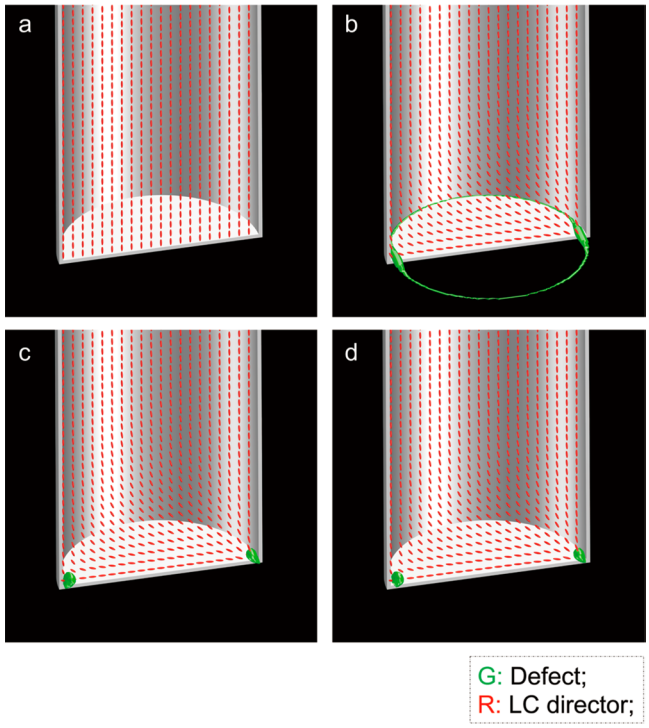

Figure 5. Landau–de Gennes numerical modeling of 5CB in a PDMS mold with different planar anchoring strength. (a) 7.74×10^{-5}, (b) 7.74×10^{-4}, (c) 7.74×10^{-3}, and (d) 3.87×10^{-2} J/m^2.

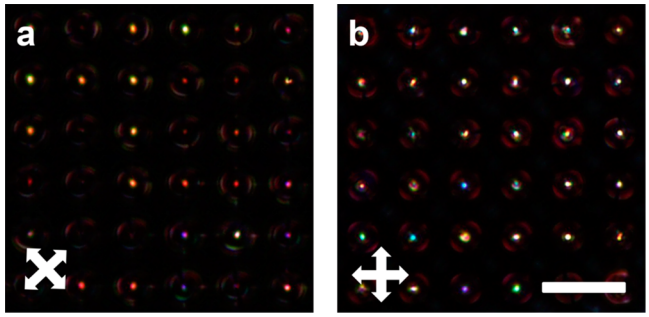

Figure 6. POM images of (a) 5CB and (b) LCM4 in a PHEMA treated PDMS mold with a pore diameter of 10 μm, a pitch of 15 μm, and a depth of 20 μm. Vertical alignments of LC molecules were observed in both LC systems. Bright dots in the pores are generated from light transmitted through the distorted LC directors at the bottom of the mold (see detailed LC director field in Figure 1b and Figure 5). Scale bar: 20 μm.

uration in PHEMA treated pores (Figure 6), we used the analogy between 5CB and LCM4 to estimate the relative planar anchoring strength of LCM4 in PHEMA coated pores as ~10^{-5} J/m^2, suggesting a relatively weak planar anchoring.

Finally, across T_{NI}, we find a relatively large strain in the radial direction (~30%) measured from the diameters in the middle of the pillars at 50 and 110 °C, respectively (Figure 4c,d). Our result is consistent with that from the strain induced in LCM4 nanofibers (~300 nm in diameter, 6 μm in length) templated from an anodic aluminum oxide (AAO) membrane with 20 mol % cross-linker.[38] Similar to PHEMA, the AAO surface is rich in hydroxyl groups, providing planar anchoring of LCM4. When the actuation of the LCM4 pillars was characterized in a top view under the bright field (BF) microscopy (Figure 4e), an average 30% radial strain was

DOI: 10.1021/acsami.6b02789
ACS Appl. Mater. Interfaces 2016, 8, 12466–12472

measured, similar to that observation from Figure 4c-d. We note that when heated above T_{NI}, the pillars tilted slightly at 110 °C, which could be attributed to the different thermal expansion coefficients between the polyurethane acrylate (PUA) supporting layer and LCM4 pillars.

CONCLUSIONS

We successfully prepared NLCE micropillars with uniform LC alignment by manipulating the surface chemistry of the PDMS mold for soft lithography. By coating the mold with PHEMA, we switched the PDMS mold surface from hydrophobic to hydrophilic, thus altering the LC anchoring from weakly homeotropic to planar for both 5CB and LCM4. In turn, highly uniform monodomains of LC alignment along the film thickness were obtained. After cross-linking LCM4 monomers imbibed in the mold, the LC director in the resulting LCE pillars was maintained, leading to a large radial strain (~30%) across T_{NI}. Compared to the application of a magnetic field to align LCMs, we believe that the ability to control interfacial chemistry on a patterned mold in soft lithography offers several distinct advantages. (1) It is, in some ways, much simpler and more elegant to direct LC alignment over a large area, specifically in the case of more complex systems, such as porous membranes, channels, and other 3D structures. (2) While the actuation behaviors of NLCE micropillars based on the same LCM have been previously studied, the strain achieved by our method is among the highest reported in literature from similar LCM systems. In the first study of LCM4 micropillars, Buguin et al.[29] reported an equivalent ~24% radial strain at 10 mol % cross-linker loading, and Cui et al.[13] showed an ~12% radial strain from the LCM4 micropillars with 45 mol % cross-linker. Recall that our LCM4 micropillars have 30% radial strain in the middle of the pillars with 20 mol % loading of the same cross-linker used by Cui et al.[13] It is clear that the 30% actuation strain in our system should be attributed to the ability to uniformly control LC director field within the channels (or pillars). (3) Our method is very versatile and can be applied to other LCM systems using a different surface coating and a wide variety of pattern geometries. By combining topography and interfacial chemistry to manipulate the boundary conditions within the micro- and nanostructures, we expect to induce a rich library of LCE actuation behaviors for a variety of potential applications, including sensors, tunable wetting and adhesion, photonic displays, and origami assembly.

ASSOCIATED CONTENT

Supporting Information

The Supporting Information is available free of charge on the ACS Publications website at DOI: 10.1021/acsami.6b02789.

Water contact angle measurement of PHEMA coated PDMS at different UV dosages, POM image of LCM4 in a nontreated PDMS mold. (PDF)

AUTHOR INFORMATION

Corresponding Author

* E-mail: shuyang@seas.upenn.edu.

Notes

The authors declare no competing financial interest.

ACKNOWLEDGMENTS

We acknowledge support by the National Science Foundation (NSF) Materials Science and Engineering Center (MRSEC) Grant to University of Pennsylvania, DMR-1120901, DMR-1410253 (S.Y.), and DMR12-62047 (R.D.K.). This work is also partially supported by a Simons Investigator grant from the Simons Foundation to R.D.K. We also acknowledge Dr. Simon Čopar for providing POV-Ray scene file generator for visualizations of numerical results. Lawrence Livermore National Laboratory is operated by Lawrence Livermore National Security, LLC, for the U.S. Department of Energy, National Nuclear Security Administration under Contract DE-AC52-07NA27344, LLNL-ABS-678248.

REFERENCES

(1) Warner, M.; Terentjev, E. M. *Liquid Crystal Elastomers*. Oxford University Press: Oxford, 2003; p 424.
(2) Spillmann, C. M.; Naciri, J.; Chen, M.-S.; Srinivasan, A.; Ratna, B. R. Tuning the Physical Properties of a Nematic Liquid Crystal Elastomer Actuator. *Liq. Cryst.* **2006**, *33*, 373−380.
(3) Thomsen, D. L.; Keller, P.; Naciri, J.; Pink, R.; Jeon, H.; Shenoy, D.; Ratna, B. R. Liquid Crystal Elastomers with Mechanical Properties of a Muscle. *Macromolecules* **2001**, *34*, 5868−5875.
(4) Li, M.-H.; Keller, P. Artificial Muscles Based on Liquid Crystal Elastomers. *Philos. Trans. R. Soc., A* **2006**, *364*, 2763−2777.
(5) Zheng, Z.-g.; Li, Y.; Bisoyi, H. K.; Wang, L.; Bunning, T. J.; Li, Q. Three-Dimensional Control of the Helical Axis of a Chiral Nematic Liquid Crystal by Light. *Nature* **2016**, *531*, 352−356.
(6) Wang, L.; Li, Q. Stimuli-Directing Self-Organized 3D Liquid-Crystalline Nanostructures: From Materials Design to Photonic Applications. *Adv. Funct. Mater.* **2016**, *26*, 10−28.
(7) Bisoyi, H. K.; Li, Q. Light-Directed Dynamic Chirality Inversion in Functional Self-Organized Helical Superstructures. *Angew. Chem., Int. Ed.* **2016**, *55*, 2994−3010.
(8) Bisoyi, H. K.; Li, Q. Light-Directing Chiral Liquid Crystal Nanostructures: From 1D to 3D. *Acc. Chem. Res.* **2014**, *47*, 3184−3195.
(9) Jin, L. H.; Lin, Y.; Huo, Y. Z. A Large Deflection Light-Induced Bending Model for Liquid Crystal Elastomers under Uniform or Non-Uniform Illumination. *Int. J. Solids Struct.* **2011**, *48*, 3232−3242.
(10) Urayama, K.; Honda, S.; Takigawa, T. Deformation Coupled to Director Rotation in Swollen Nematic Elastomers under Electric Fields. *Macromolecules* **2006**, *39*, 1943−1949.
(11) van Oosten, C. L.; Bastiaansen, C. W. M.; Broer, D. J. Printed Artificial Cilia from Liquid-Crystal Network Actuators Modularly Driven by Light. *Nat. Mater.* **2009**, *8*, 677−682.
(12) Ohm, C.; Brehmer, M.; Zentel, R. Liquid Crystalline Elastomers as Actuators and Sensors. *Adv. Mater.* **2010**, *22*, 3366−3387.
(13) Cui, J.; Drotlef, D.-M.; Larraza, I.; Fernández-Blázquez, J. P.; Boesel, L. F.; Ohm, C.; Mezger, M.; Zentel, R.; del Campo, A. Bioinspired Actuated Adhesive Patterns of Liquid Crystalline Elastomers. *Adv. Mater.* **2012**, *24*, 4601−4604.
(14) Liu, D.; Bastiaansen, C. W. M.; den Toonder, J. M. J.; Broer, D. J. Photo-Switchable Surface Topologies in Chiral Nematic Coatings. *Angew. Chem., Int. Ed.* **2012**, *51*, 892−896.
(15) Ge, J.; Hu, Y.; Yin, Y. Highly Tunable Superparamagnetic Colloidal Photonic Crystals. *Angew. Chem.* **2007**, *119*, 7572−7575.
(16) Sato, O.; Kubo, S.; Gu, Z.-Z. Structural Color Films with Lotus Effects, Superhydrophilicity, and Tunable Stop-Bands. *Acc. Chem. Res.* **2009**, *42*, 1−10.
(17) Kim, H.; Ge, J.; Kim, J.; Choi, S.-e.; Lee, H.; Lee, H.; Park, W.; Yin, Y.; Kwon, S. Structural Colour Printing Using a Magnetically Tunable and Lithographically Fixable Photonic Crystal. *Nat. Photonics* **2009**, *3*, 534−540.
(18) Li, J.; Shim, J.; Deng, J.; Overvelde, J. T. B.; Zhu, X.; Bertoldi, K.; Yang, S. Switching Periodic Membranes via Pattern Transformation and Shape Memory Effect. *Soft Matter* **2012**, *8*, 10322−10328.
(19) Lee, E.; Zhang, M.; Cho, Y.; Cui, Y.; Van der Spiegel, J.; Engheta, N.; Yang, S. Tilted Pillars on Wrinkled Elastomers as a

Reversibly Tunable Optical Window. *Adv. Mater.* **2014**, *26*, 4127−4133.
(20) Ge, D.; Lee, E.; Yang, L.; Cho, Y.; Li, M.; Gianola, D. S.; Yang, S. A Robust Smart Window: Reversibly Switching from High Transparency to Angle-Independent Structural Color Display. *Adv. Mater.* **2015**, *27*, 2489−2495.
(21) Glassmaker, N. J.; Jagota, A.; Hui, C.-Y.; Kim, J. Design of Biomimetic Fibrillar Interfaces: 1. Making Contact. *J. R. Soc., Interface* **2004**, *1*, 23−33.
(22) Lin, P. C.; Vajpayee, S.; Jagota, A.; Hui, C. Y.; Yang, S. Mechanically Tunable Dry Adhesive from Wrinkled Elastomers. *Soft Matter* **2008**, *4*, 1830−1835.
(23) Kamperman, M.; Kroner, E.; del Campo, A.; McMeeking, R. M.; Arzt, E. Functional Adhesive Surfaces with "Gecko" Effect: The Concept of Contact Splitting. *Adv. Eng. Mater.* **2010**, *12*, 335−348.
(24) Krupenkin, T. N.; Taylor, J. A.; Schneider, T. M.; Yang, S. From Rolling Ball to Complete Wetting: The Dynamic Tuning of Liquids on Nanostructured Surfaces. *Langmuir* **2004**, *20*, 3824−3827.
(25) Lin, P.-C.; Yang, S. Mechanically Switchable Wetting on Wrinkled Elastomers with Dual-Scale Roughness. *Soft Matter* **2009**, *5*, 1011−1018.
(26) Chen, C.-M.; Yang, S. Directed Water Shedding on High-Aspect-Ratio Shape Memory Polymer Micropillar Arrays. *Adv. Mater.* **2014**, *26*, 1283−1288.
(27) Yu, Y.; Ikeda, T. Soft Actuators Based on Liquid-Crystalline Elastomers. *Angew. Chem., Int. Ed.* **2006**, *45*, 5416−5418.
(28) Woltman, S. J.; Jay, G. D.; Crawford, G. P. Liquid-Crystal Materials Find a New Order in Biomedical Applications. *Nat. Mater.* **2007**, *6*, 929−938.
(29) Buguin, A.; Li, M.-H.; Silberzan, P.; Ladoux, B.; Keller, P. Micro-Actuators: When Artificial Muscles Made of Nematic Liquid Crystal Elastomers Meet Soft Lithography. *J. Am. Chem. Soc.* **2006**, *128*, 1088−1089.
(30) Yang, H.; Buguin, A.; Taulemesse, J.-M.; Kaneko, K.; Mery, S.; Bergeret, A.; Keller, P. Micron-Sized Main-Chain Liquid Crystalline Elastomer Actuators with Ultralarge Amplitude Contractions. *J. Am. Chem. Soc.* **2009**, *131*, 15000−15004.
(31) Meyer, R. B. On the Existence of Even Indexed Disclinations in Nematic Liquid Crystals. *Philos. Mag.* **1973**, *27*, 405−424.
(32) Zhang, Y.; Lo, C.-W.; Taylor, J. A.; Yang, S. Replica Molding of High-Aspect-Ratio Polymeric Nanopillar Arrays with High Fidelity. *Langmuir* **2006**, *22*, 8595−8601.
(33) Cavallaro, M.; Gharbi, M. A.; Beller, D. A.; Čopar, S.; Shi, Z.; Baumgart, T.; Yang, S.; Kamien, R. D.; Stebe, K. J. Exploiting Imperfections in the Bulk to Direct Assembly of Surface Colloids. *Proc. Natl. Acad. Sci. U. S. A.* **2013**, *110*, 18804−18808.
(34) Kleman, M.; Laverntovich, O. D. *Soft Matter Physics: An Introduction*. Springer: New York, 2003; p 140.
(35) Wei, R. B.; Zhou, L. Y.; He, Y. N.; Wang, X. G.; Keller, P. Effect of Molecular Parameters on Thermomechanical Behavior of Side-On Nematic Liquid Crystal Elastomers. *Polymer* **2013**, *54*, 5321−5329.
(36) Gennes, P.-G. d. *The Physics of Liquid Crystals*. Clarendon: Oxford, 1974.
(37) Lee, J. N.; Park, C.; Whitesides, G. M. Solvent Compatibility of Poly(dimethylsiloxane)-Based Microfluidic Devices. *Anal. Chem.* **2003**, *75*, 6544−6554.
(38) Ohm, C.; Haberkorn, N.; Theato, P.; Zentel, R. Template-Based Fabrication of Nanometer-Scaled Actuators from Liquid-Crystalline Elastomers. *Small* **2011**, *7*, 194−198.

DOI: 10.1021/acsami.6b02789
ACS Appl. Mater. Interfaces 2016, 8, 12466−12472